

3-colorable planar graphs have an intersection segment representation using 3 slopes*

Daniel Gonçalves^a

^a*LIRMM, Université de Montpellier, CNRS, Montpellier, France.*

Abstract

In his PhD Thesis E.R. Scheinerman conjectured that planar graphs are intersection graphs of line segments in the plane. This conjecture was proved with two different approaches by J. Chalopin and the author, and by the author, L. Isenmann, and C. Pennarun. In the case of 3-colorable planar graphs E.R. Scheinerman conjectured that it is possible to restrict the set of slopes used by the segments to only 3 slopes. Here we prove this conjecture by using an approach introduced by S. Felsner to deal with contact representations of planar graphs with homothetic triangles.

1 Introduction

In this paper, we consider intersection representations for planar graphs. A *segment representation* of a graph G maps every vertex $v \in V(G)$ to a straight line segment \mathbf{v} of the plane so that two segments \mathbf{u} and \mathbf{v} intersect if and only if $uv \in E(G)$. In his PhD Thesis, E.R. Scheinerman [15] conjectured that every planar graph has a segment representation. This conjecture attracted a lot of attention. H. de Fraysseix and P. Ossona de Mendez [6] proved it for a large family of planar graphs, the planar graphs having a 4-coloring in which every induced cycle of length 4 uses at most 3 colors. In particular, this implies the conjecture for 3-colorable planar graphs. Then J. Chalopin and the author finally proved this conjecture [2]. More recently, a much simpler proof was provided by the author, L. Isenmann, and C. Pennarun [10]. Here we focus on segment representations of planar graphs with further restrictions.

In his PhD Thesis, E.R. Scheinerman [15] proved that every outerplanar graph has a segment representation where only 3 slopes are used, and where parallel segments do not intersect. Let us call such a representation a *3-slopes segment representation*. This result led E.R. Scheinerman conjecture [16] (see also [6]) that such representation exists for every 3-colorable planar graph. Later, several groups proved a related result on bipartite planar graphs [3, 7, 11]. They proved that every bipartite planar graph has

*This is the extended version of a paper presented at WG '19 [8]. This research is partially supported by the ANR GATO, under contract ANR-16-CE40-0009.

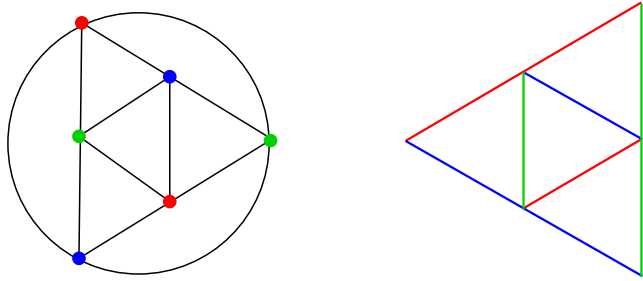


Figure 1: The octahedron and a 3-slopes contact representation. It is unique, up to vertex automorphism, up to scaling, and once the slopes are set.

a 2-slopes segment representation, with the extra property that segments do not cross each other. Let us call such a representation a *2-slopes contact segment representation*. Later, de Castro *et al.* [1] considered a particular class of 3-colorable planar graphs. They proved that every triangle-free planar graph has a 3-slopes contact segment representation. Such a contact segment representation cannot be asked for any 3-colorable planar graph. Indeed, up to isomorphism, the octahedron has only one 3-slopes contact segment representation depicted in Figure 1, and one can easily check that this representation does not extend to the (3-colorable) graph obtained after gluing a copy of an octahedron in each of its faces. However, we will use 3-slopes contact segment representations in the proof of our main result.

Theorem 1 *Every 3-colored planar graph has a 3-slopes segment representation such that parallel segments correspond to the color classes.*

As such a representation implies 3-colorability, and as 3-colorability is NP-complete already for planar graphs [17] we have that it is NP-hard to decide if a plane graphs has a 3-slopes segment representation in which no parallel segments intersect. Here, the NP-membership clearly follows from Theorem 1. The NP-membership is often non-trivial for segment representations. For example, we know that it is NP-hard to decide whether a graph G admits a segment representation, actually it is even $\exists\mathbb{R}$ -complete [13], but it is still open whether this problem belongs to NP or not.

It is easy to see that every 3-colored planar graph is the induced subgraph of some 3-colored triangulation. Indeed, adding a new vertex in a non-triangular face, one can reduce the maximum length of such a face, or reduce the number of colors around such a face. As a 3-slopes segment representation of a triangulation naturally induces such a representation for its induced subgraphs, we can restrict ourselves to the case of triangulations in the following. In Section 2 we provide some basic definitions. Section 3 is devoted to the so-called *triangular contact schemes*, which are particular 3-slopes contact segment representations of an auxiliary graph (to be formally defined there). It is shown that every 3-colorable triangulation admits such a scheme. Then, those schemes are used in Section 4 to build 3-slopes segment representations. Finally, we conclude with some remarks on 4-slopes segment representations.

2 Terminology

All graphs considered here are simple, that is without loops nor multiple edges. A *triangulation* is a plane graph where every face has size three. A triangulation T is *Eulerian* if every vertex has even degree. It is well known that these triangulations are the 3-colorable triangulations [14]. Actually, these triangulations are uniquely 3-colorable (up to color permutation). Hence, their vertex set $V(T)$ is canonically partitioned into three independent sets A , B and C . In the following we will denote the vertices of these sets respectively a_i with $0 \leq i < |A|$, b_j with $0 \leq j < |B|$, and c_k with $0 \leq k < |C|$. In such a triangulation T any face is incident to one vertex a_i , one vertex b_j , and one vertex c_k , and these vertices appear in this order either clockwise or counterclockwise. In the following, the vertices of the outerface are always denoted by a_0 , b_0 and c_0 , and they appear clockwise in this order around T . As the orders of two adjacent faces are opposite, the dual graph of T is bipartite. Given a Eulerian triangulation T with face set $F(T)$, let us denote by $F_1(T)$ and $F_2(T)$ (or simply F_1 and F_2 if it is clear from the context) the face sets partitioning $F(T)$, such that no two adjacent faces belong to the same set, and such that $F_2(T)$ contains the outer face. Note that by construction for any face $f \in F_1(T)$ (resp. $f \in F_2(T)$) its vertices a_i , b_j and c_k appear in clockwise (resp. counterclockwise) order around f . Note that the vertices a_0 , b_0 and c_0 appear in clockwise order around T , but in counterclockwise order with respect to the outer face. Let $n = |V(T)|$. As T is a triangulation, by Euler's formula it has $2n - 4$ faces. Hence, as T 's dual is bipartite and 3-regular, $|F_1(T)| = |F_2(T)| = n - 2$.

In the following, we build 3-slopes segment representations. The 3 slopes used are expected to be distinct, but apart from that the exact 3 slopes considered do not matter. Indeed, for any two triples of slopes, (s_1, s_2, s_3) and (s'_1, s'_2, s'_3) , there exists an affine map of the plane turning any 3-slopes segment representation using slopes (s_1, s_2, s_3) into a 3-slopes segment representation using slopes (s'_1, s'_2, s'_3) . We denote by \vec{a} , \vec{b} , and \vec{c} the vectors corresponding to slopes of the sets A , B , and C respectively. The magnitude of these vectors is chosen such that $\vec{a} + \vec{b} + \vec{c} = \vec{0}$.

3 TC-representations and TC-schemes

We begin with the definition of the particular type of 3-slopes contact representations illustrated in Figure 2.

Definition 2 For the fixed vectors \vec{a} , \vec{b} , \vec{c} as defined previously, a Triangular 3-slopes Contact segment representation (TC-representation for short) is a 3-slopes contact segment representation using the same slopes as \vec{a} , \vec{b} , and \vec{c} , and where:

- Three segments \mathbf{a}_0 , \mathbf{b}_0 , and \mathbf{c}_0 , form a triangle which contains all the other segments. Going clockwise around this outer-triangle, one successively follows $\alpha \vec{a}$, $\alpha \vec{b}$, and then $\alpha \vec{c}$, with $\alpha = 1$.
- Every inner region is a triangle, where each side is contained in a segment of the representation.

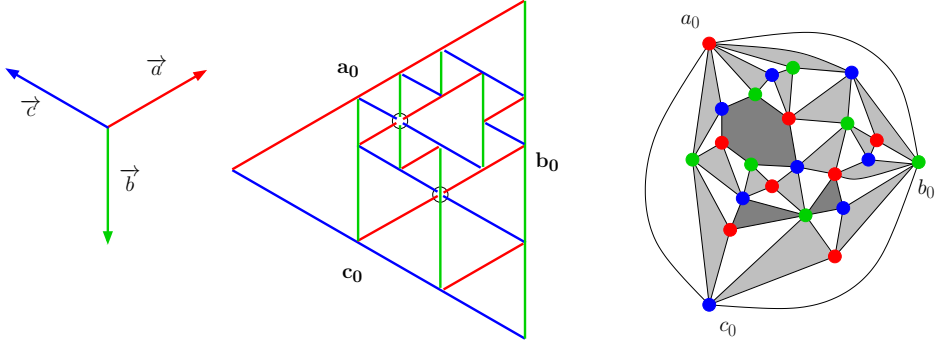


Figure 2: (left) Vectors \vec{a} , \vec{b} , and \vec{c} (middle) A TC-representation \mathcal{R} with various types of intersection points. The circled ones correspond to particular intersection points with more than three segments. (right) Its corner graph $C(\mathcal{R})$, where gray faces correspond to the degenerate faces (i.e. they correspond to intersection points in \mathcal{R}). The dark gray faces are particular degenerate faces. One has size six, and there are two faces of size three that correspond to the same intersection point.

- Two parallel segments intersect in at most one point, and this point is an endpoint of both segments.

Remark 3 In such a representation, an intersection point \mathbf{p} is of one of the following four types (see Figure 2).

- The intersection point of 2 outer segments;
- the intersection point of 3 segments (with 3 distinct slopes) such that exactly two of them end at \mathbf{p} ;
- the intersection point of 5 segments such that exactly four of them end at \mathbf{p} (such a point will be generally considered as the merge of two intersection points of 3 segments); or
- the intersection point of 6 segments that have an end at \mathbf{p} .

Definition 4 Given a TC-representation \mathcal{R} , let the corner graph $C(\mathcal{R})$ be the plane graph whose vertices correspond to the segments of the representation, and where two vertices are adjacent if and only if the corresponding segments form a corner of one of the inner triangles. The orders of the neighbors around a vertex v correspond to the order of the segments around the segment \mathbf{v} .

Note that the corner graph of a TC-representation has several properties. For example, since two parallel segments cannot form a corner of a triangle, they correspond to non-adjacent vertices. The slopes hence define a 3-coloring of the graph. Note also that the dual graph of $C(\mathcal{R})$ is bipartite. Indeed, such a plane graph has two types of

faces, one set contains the (triangular) faces corresponding to the inner regions of the TC-representation, and the other set contains the outerface and the faces corresponding to intersection points. Let us denote the latter faces *degenerate faces*, and note that those faces have size three or six. A size six face $(a_i, b_j, c_k, a_{i'}, b_{j'}, c_{k'})$ comes from the intersection point of six segments, and as those six segments go in distinct directions they do not intersect elsewhere, so this cycle has no chord in $C(\mathcal{R})$. Note that going clockwise on the border of any inner region of \mathcal{R} , since $\vec{a} + \vec{b} + \vec{c} = \vec{0}$, one successively follows $\alpha \vec{a}$, $\alpha \vec{b}$, and then $\alpha \vec{c}$, for some not necessarily positive value α . This value α is the *size* of this inner triangle. Note that the outer-triangle formed by a_0, b_0 and c_0 has size 1. In our illustrations, the triangles of positive size have a corner on the left. Let us now prove that any corner graph is 3-connected.

Lemma 5 *For any TC-representation \mathcal{R} , its corner graph $C(\mathcal{R})$ is 3-connected, and hence it has only one planar embedding with a_0, b_0, c_0 on the outerboundary in clockwise order.*

Proof. Towards a contradiction, suppose $C(\mathcal{R})$ is not 3-connected for some TC-representation \mathcal{R} , and let $\{x, y\}$ be a separating set. The case where there is a vertex cut but no separating set of size two is trivial. We assume without loss of generality that x is a *A*-vertex, then by symmetry we just have to consider the case where y is a *A*-vertex, and the case where y is a *C*-vertex.

If both x and y are *A*-vertices, let us prove that any connected component H of $C(\mathcal{R}) \setminus \{x, y\}$ contains b_0 . Indeed, let b_j be the rightmost vertical segment of H . If $b_j \neq b_0$ there is a *C*-vertex c_k such that c_k intersects b_j on its topmost point and such that c_k continues further on the right. Indeed, the topmost inner triangle incident to the right of b_j is incident to such segment c_k . Then the rightmost point of c_k has to belong to some vertical segment on the right of b_j , a contradiction.

If x is a *A*-vertex and y is a *C*-vertex, we have to distinguish two subcases according to how they intersect (or not).

Suppose first that x and y are not on the boundary of an inner triangle, of negative size (i.e. pointing to the right). In this case, we can proceed as in the previous case by considering the rightmost vertical segment of any connected component H of $C(\mathcal{R}) \setminus \{x, y\}$. If $b_j \neq b_0$, the segment b_j has (at least) $2t$ incident segments going further to the right, where $t \geq 1$ is the number of inner faces incident to b_j , on its right. If some of these $2t$ neighbors in $C(\mathcal{R})$ is distinct from x and y , this segment brings us to another *B*-vertex on the right, as in the previous case. If these $2t$ neighbors correspond exactly to x and y , we have $t = 1$ and we are in the case where x and y are on the boundary of an inner triangle, of negative size, a contradiction.

Suppose now that x and y are on the boundary of an inner triangle, of negative size (i.e. pointing to the right). In that case, we are going to prove that any connected component H of $C(\mathcal{R}) \setminus \{x, y\}$ contains the vertex b_t , corresponding to the leftmost vertical segment; the one forming an inner triangle with a_0 and c_0 . We proceed similarly as above by letting b_j be the leftmost vertical segment of H , and by considering its (at least) $2t$ incident segments going further to the left, where $t \geq 1$ is the number of inner faces incident to b_j , on its left. If some of these neighbors in $C(\mathcal{R})$ is distinct from x and y , this segment would bring us to another *B*-vertex on the left, a contradiction. We are thus left with the case where $t = 1$ and where there are only two such

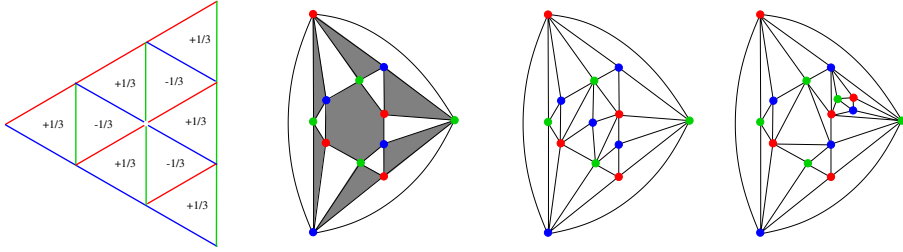


Figure 3: From left to right. A TC-representation \mathcal{R} , with the size of its inner triangles; its corner graph $C(\mathcal{R})$, where gray faces are the degenerate faces; and two triangulations where \mathcal{R} is a TC-scheme of both.

neighbors, which would be x and y . This is impossible because in that case x and y would be on the boundary of an inner triangle, of positive size, and it is impossible in a TC-representation for two segments to have more than one inner triangle in common. \square

Lemma 6 *Consider a Eulerian triangulation T and a TC-representation \mathcal{R} such that each segment of \mathcal{R} corresponds to a distinct vertex of T . The following two statements are equivalent:*

- (1) *$C(\mathcal{R})$ is a submap of T with the same outer face as T , such that the vertices and edges of T not in $C(\mathcal{R})$ lie inside degenerate faces of $C(\mathcal{R})$.*
- (2) *The outerface and the non-degenerate faces of $C(\mathcal{R})$ are, respectively, the outerface and a subset of the inner faces of T .*

If (1) (or equivalently (2)) is fulfilled, we call \mathcal{R} a *TC-scheme* of T (see Figure 3).

Proof. In both cases, the outerfaces of $C(\mathcal{R})$ and T are asked to be the same, so we can focus on the inner faces.

(1) \implies (2). If $C(\mathcal{R})$ and T fulfill (1), then any non-degenerate face of $C(\mathcal{R})$ induces a cycle in T (as $C(\mathcal{R})$ is a subgraph of T). Furthermore, this cycle does not contain any edge or vertex of T . It thus bounds an inner face of T .

(2) \implies (1). In a corner graph $C(\mathcal{R})$, every edge belongs to a non-degenerate inner-face (by definition). Hence, if $C(\mathcal{R})$ and T fulfill (2), any edge of $C(\mathcal{R})$ is an edge of T . $C(\mathcal{R})$ is thus a subgraph of T . Furthermore, as they have same outerface, and as $C(\mathcal{R})$ has only one possible embedding (by Lemma 5) we have that $C(\mathcal{R})$ is a submap of T . The non-degenerate faces of $C(\mathcal{R})$ being inner faces of T (by (2)) the vertices and edges of T not in $C(\mathcal{R})$ have to lie inside the degenerate faces of $C(\mathcal{R})$. \square

The main ingredient in the proof of Theorem 1 is the following.

Theorem 7 *Every Eulerian triangulation T has a TC-scheme, and this scheme is unique.*

To prove this theorem we use TC-schemes as defined in Lemma 6.(2). The definition in Lemma 6.(1) will be used in Section 4 to complete the proof of Theorem 1. To prove Theorem 7, we first model TC-schemes of T by means of a system of linear equations in Subsection 3.1. We then show in Subsection 3.2 that such a linear system always has a solution, and that this solution is unique (c.f. Lemma 8). Finally, we show in Subsection 3.3 that the solution of this linear system defines a TC-scheme of T (c.f. Lemma 11).

3.1 The linear system model

In a TC-representation all the triangles are homothetic, and they are included in the outer triangle which has size one. Note that we will have positive, negative, and degenerate (zero) homothets. Recall that the size of a triangle is its relative size with respect to the outer triangle. The variables of our linear system correspond to the sizes of the triangular regions. So for each face $f \in F_1$ we have a variable x_f . Informally, the value of x_f will prescribe the size and shape of the corresponding triangle in a TC-representation. If $x_f < 0$, $x_f = 0$, or if $x_f > 0$ the corresponding triangle has a corner on the right, is missing, or has a corner on the left, respectively.

Let us denote by $F_1(v)$ the subset of faces of F_1 incident to v . As the outer triangle has size 1 and contains the other triangles, the faces in $F_1(a_0)$ should have non-negative sizes, and they should sum up to 1 (see Figure 4, left). We hence consider the following constraint.

$$\sum_{f \in F_1(a_0)} x_f = 1 \quad (a_0)$$

We add no constraint about the sign of these sizes. Note that similar constraints hold for b_0 and c_0 .

$$\sum_{f \in F_1(b_0)} x_f = 1 \quad (b_0)$$

$$\sum_{f \in F_1(c_0)} x_f = 1 \quad (c_0)$$

Similarly, around an inner segment of a TC-representation all the triangles on one side have the same size sign, which is opposite to the other side (see Figure 4, right). Furthermore, by summing all of these sizes one should obtain 0. Hence, for any inner vertex u we consider the following constraint.

$$\sum_{f \in F_1(u)} x_f = 0 \quad (u)$$

In the following, Equation (a_j) will refer to Equation (u) where vertex u is replaced by a_j . Note that every face $f \in F_1$ is incident to exactly one vertex of A , one vertex of B , and one vertex of C . Hence by summing Equations $(a_0), (a_1), \dots, (a_{|A|})$, one obtains that $\sum_{f \in F_1} x_f = 1$. The same holds with Equations $(b_0), (b_1), \dots, (b_{|B|})$, or

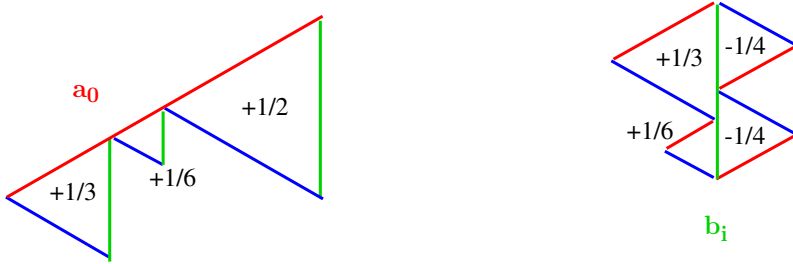


Figure 4: (left) The size of the triangles around a_0 . (right) The size of the triangles around some inner vertex b_i .

with Equations (c_0) , $(c_1), \dots, (c_{|C|})$. Equations (b_0) and (c_0) are hence implied by the others, and thus we do not need to consider them anymore. Let us denote by \mathcal{L} the obtained system of $n - 2$ linear equations on $|F_1| = n - 2$ variables.

3.2 \mathcal{L} has a unique solution

Let us define the set $V' = V \setminus \{b_0, c_0\}$ of size $n - 2$. Finding a solution to \mathcal{L} is equivalent to finding a vector $S \in \mathbb{R}^{F_1}$ (that is a vector indexed by elements of F_1) such that $MS = I$, where $M \in \mathbb{R}^{V' \times F_1}$ (a square matrix indexed by elements of $V' \times F_1$) and $I \in \mathbb{R}^{V'}$ are defined by

$$M(x_i, f) = \begin{cases} 1 & \text{if } f \in F_1(x_i) \\ 0 & \text{otherwise.} \end{cases} \quad I(x_i) = \begin{cases} 1 & \text{if } x_i = a_0 \\ 0 & \text{otherwise.} \end{cases}$$

Given some bijective mappings $g_{V'} : [1, \dots, n - 2] \rightarrow V'$ and $g_{F_1} : [1, \dots, n - 2] \rightarrow F_1$, one can index the elements of M by pairs $(i, j) \in [1, \dots, n - 2] \times [1, \dots, n - 2]$, and thus define the determinant of M . By the following lemma, \mathcal{L} has a solution vector S , and this solution is unique.

Lemma 8 *The matrix M is non-degenerate, i.e. $\det(M) \neq 0$.*

The proof of this lemma is inspired by the work of S. Felsner [4] on contact representations with homothetic triangles. See also [5] for another proof using the same approach.

Proof. Let T_M be the bipartite graph with independent sets V' and F_1 such that $v \in V'$ and $f \in F_1$ are adjacent if and only if v and f are incident in T . Note that M is the biadjacency matrix of T_M . From the embedding of T one can easily embed T_M in such a way that all the inner faces have size 6, and such that a_0 is on the outerboundary.

Note that every perfect matching of T_M (if any) corresponds to a permutation σ on $[1, \dots, n - 2]$ defined by $\sigma(g_{V'}^{-1}(v)) = g_{F_1}^{-1}(f)$, for any edge vf of the perfect matching. If the obtained permutation is even we call such perfect matching positive, otherwise it is negative. From the Leibniz formula for the determinant,

$$\det(M) = \sum_{\sigma \in S_{n-2}} \text{sgn}(\sigma) \prod_{i \in [1, \dots, n-2]} M(g_{V'}(i), g_{F_1}(\sigma(i)))$$

one can see that $\det(M)$ counts the number of positive perfect matchings of T_M minus its number of negative perfect matchings.

Claim 9 *The graph T_M admits at least one perfect matching.*

Proof. As T_M is bipartite, and as $|V'| = |F_1|$, it suffices to show that T_M has an F_1 -saturating matching. This follows from Hall's marriage theorem, and the fact that for any set $X \subseteq F_1$ the set $Y \subset V'$ of vertices incident to a face in X is such that $|Y| \geq |X|$. Let us show this below for any set $X \subseteq F_1$.

Consider the (planar) subgraph of T with all the edges and all the vertices incident to a face of X . Then, triangulate this graph and denote by T_X the obtained triangulation. Note that as any two faces of X are not adjacent in T_X , this triangulation has at least $2|X|$ faces. Indeed, around each vertex there are at least twice as many faces as faces of X , and summing over every vertex one obtains the inequality. Together with the fact that T_X has $2|V(T_X)| - 4$ faces,

$$2|V(T_X)| - 4 \geq 2|X|$$

and that $V(T_X) \subseteq Y \cup \{b_0, c_0\}$,

$$|Y| + 2 \geq |V(T_X)|$$

one obtains that

$$2|V(T_X)| - 4 + 2|Y| + 4 \geq 2|X| + 2|V(T_X)|$$

$$|Y| \geq |X|$$

□

Given a graph G and a perfect matching M of G , an *alternating cycle* C is a cycle of G with edges alternating between M and $E(G) \setminus M$. Note that replacing in M the edges of $M \cap C$ by the edges of $C \setminus M$ yields another perfect matching. We call such operation a *cycle exchange*. It is folklore that the perfect matchings of a graph are linked by cycle exchanges. Indeed, given any perfect matching M_1 of G one can reach any perfect matching M_2 , by a succession of cycle exchanges. Actually, for T_M any such cycle has length congruent to $2 \pmod{4}$.

Claim 10 *For any perfect matching of T_M and any of its alternating cycles C , we have that the length $\ell(C)$ of C is congruent to $2 \pmod{4}$.*

Proof. The subgraph G of T_M induced by the vertices and edges on or inside C is such that all the inner faces have length 6, and it is routine from Euler's formula to show that C has length congruent to $2 + 2|V_G| \pmod{4}$, where V_G is the vertex set of G . Indeed,

$$\begin{aligned} \ell(C) - 6 + 6|F_G| &= \sum_{f \in F_G} \ell(f) = 2|E_G| = 2|V_G| + 2|F_G| - 4 \\ \ell(C) &\equiv 2|V_G| + 2 \pmod{4} \end{aligned}$$

Finally, as the vertices of G are paired by the perfect matching we have that $|V_G|$ is even. \square

The previous claim implies that all the perfect matchings of T_M induce permutations of the same sign. Indeed, performing a $(4k+2)$ -cycle exchange does not change the sign of the permutation, as it corresponds to performing $2k$ transpositions in the permutation. Hence, all the terms of $\det(M)$ have the same sign, and this sum has at least one non-zero term (by Claim 9). Thus $\det(M) \neq 0$. \square

3.3 A solution of \mathcal{L} defines a TC-scheme

A TC-scheme \mathcal{R} corresponds to a solution of \mathcal{L} , the linear system defined for a Eulerian triangulation T , if \mathcal{R} is a TC-scheme of T such that each face $f \in F_1$ corresponds to an inner triangle of \mathcal{R} of size x_f , the solution of \mathcal{L} , unless $x_f = 0$. In other words, the inner regions of \mathcal{R} correspond to non-zero valued faces of F_1 .

Let us now proceed to the main result of this section.

Lemma 11 *Every Eulerian triangulation T admits a TC-scheme \mathcal{R} that corresponds to the solution of its linear system \mathcal{L} .*

Proof. We proceed by induction on the number of faces $f \in F_1$ such that $x_f = 0$. We start with the case where every face $f \in F_1$ is such that $x_f \neq 0$.

If every face $f \in F_1$ is such that $x_f \neq 0$, we construct a TC-scheme \mathcal{R} corresponding to the solution of \mathcal{L} as follows. First let Δ be a triangle formed by three vectors \vec{a} , \vec{b} , and \vec{c} in this order. The sides of Δ correspond to \mathbf{a}_0 , \mathbf{b}_0 , and \mathbf{c}_0 , respectively. For each face $f \in F_1$, let Δ_f be a homothetic copy of Δ with ratio x_f . The triangle Δ_f is thus obtained by following the vectors $x_f \vec{a}$, $x_f \vec{b}$, and $x_f \vec{c}$ in this order. We are going to show that all these triangles Δ_f can be arranged as a tiling of Δ , forming a TC-representation of T (i.e. such that $T = C(\mathcal{R})$).

Note that a necessary condition for this to work is that (1) every face of $f \in F_1$ around a_0 , b_0 , or c_0 is positive (i.e. $x_f > 0$), and that (2) for any inner vertex v of T its positive (resp. negative) incident faces in F_1 are consecutive around v . Otherwise, this would result in overlapping triangles Δ_f (see Figure 4). We first show that (1) and (2) are fulfilled, and then we show that this suffices to ensure the construction of \mathcal{R} .

Consider the incidence graph I , between vertices of $V(T)$ and faces of F_2 . First note that this plane graph has only size six faces and that they are in bijection with the faces in F_1 . Let us orient the edges of I as follows. An edge vf of I , with $v \in V(T)$ and $f \in F_2(T)$, is oriented from v to f if and only if the incident faces (which correspond to faces in F_1) have different signs. Note that for an inner vertex of T , $d^+(v) = 2k$ for some $k \geq 1$ (as v is incident to positive and to negative faces in T), and that $d^+(f) = 1$ or 3 for a face $f \in F_2$. The graph I has $2n - 2$ vertices (3 outer vertices of T , $n - 3$ inner vertices of T , and $n - 2$ faces of F_2) and $3n - 6$ edges. The outerface f^o of T has outdegree 3 in I . Otherwise, among the three faces of F_1 incident to a_0b_0 , a_0c_0 , or b_0c_0 there would be positive ones and negative ones. This would imply that two of a_0 , b_0 , and c_0 have outdegree at least 2 in I . This would be

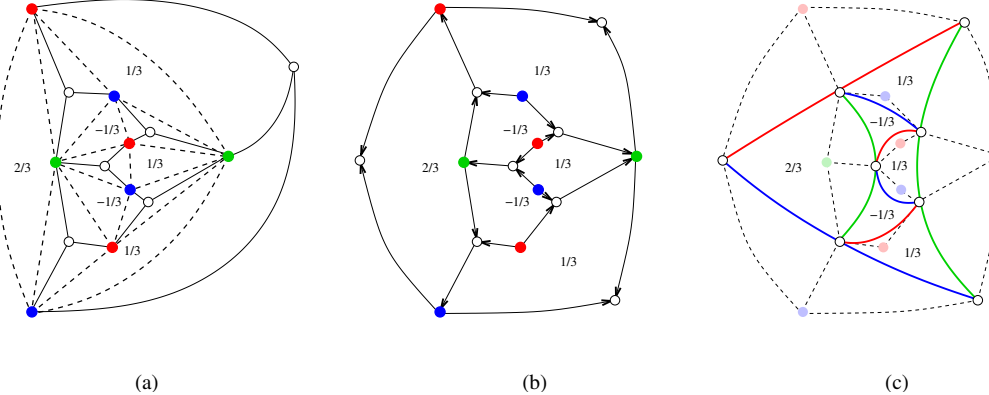


Figure 5: (a) Example of a Eulerian triangulation T (dashed lines), with incidence graph I . The numbers correspond to the solution of \mathcal{L} . (b) The graph I' obtained after (Step 1). (C) The graph G^Δ .

impossible as summing over the outdegrees of a_0, b_0, c_0 , the inner vertices of T , and the faces of $F_2(T)$ would lead to $2 + 2 + 2(n - 3) + (n - 2) > 3n - 6$. We thus have that $d^+(f^o) = 3$, and a counting argument gives us that the other faces f of F_2 have outdegree one, that the outer vertices have outdegree zero, and that the inner vertices of T have outdegree two. Thus, (1) and (2) are verified.

To construct the TC-representation of T , we define a plane graph G^Δ from I by replacing f^o with three vertices (Step 1), and for each vertex $v \in V(T)$, by turning its neighborhood in I from a star into a path (Step 2).

(Step 1) The vertex f^o is replaced by three new vertices f_a^o, f_b^o , and f_c^o in such a way that f_a^o is adjacent to b_0 and c_0 (see Figure 5). The six new edges are oriented towards the newly created vertices. Let us use I' to denote this new oriented graph. Note that now every vertex $v \in V(T)$ has outdegree two, and that by assigning size -1 to the outerface, all faces incident to v sum up to zero.

(Step 2) For each vertex $v \in V(T)$, its neighborhood in I' is turned into a path P_v whose ends are the out-neighbors of v . The in-neighbors are ordered as follows in P_v . We first denote by f^+ (resp. f^-) the out-neighbors of v such that the face following f^+ (resp. f^-), around v in clockwise order, has positive (resp. negative) size (*i.e.* solution in \mathcal{L}). Two in-neighbors f, f' of v are ordered along P_v in such a way that f is closer to f^+ than f' , if and only if the sum of the face sizes going around v from f^+ to f is lower than the sum from f^+ to f' . If the two sums are equal, then f and f' are merged into a single vertex (see Figure 6). As all the faces around v have non-zero sizes, and as positive sizes are consecutive, a vertex f is merged at most once while constructing P_v . Note that f is merged with another face f' on P_v only if vf is oriented towards v and this occurs for only one neighbor of f , so f is not merged to more faces while

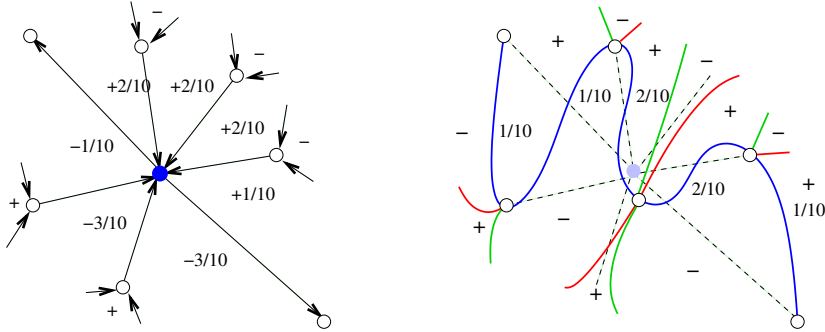


Figure 6: An example of (Step 2) with a merge of f and f' .

constructing the other paths P_u .

The obtained plane graph is denoted by G^Δ . Note that the inner faces of G^Δ correspond to faces of F_1 , and we assign them the corresponding sizes. Note also that a face of G^Δ corresponding to the face $a_i b_j c_k \in F_1$, is bordered by three subpaths of paths P_{a_i} , P_{b_j} , and P_{c_k} . We now assign a positive length to each edge of G^Δ so that the length of each of these subpaths corresponds to the size of the face, forgetting the sign. For each edge ff' of a path P_v , we assign the absolute value of the sum of the face sizes between f and f' around v in I' .

By construction, G^Δ has three types of vertices:

- The vertices f_a^o , f_b^o , and f_c^o , which have degree two. Indeed, *e.g.* the vertex f_a^o is at the end of P_{b_0} and P_{c_0} .
- The vertices originating from a single vertex $f \in V(I) \setminus (V(T) \cup \{f^o\})$. As each such f has in-degree two and out-degree one in I , it is at the end of two paths and in the middle of a third one.
- The vertices originating from two vertices $f, f' \in V(I) \setminus (V(T) \cup \{f^o\})$. By construction, such vertex is in the middle of a path, and has two paths ending on each side (corresponding to in-neighbors in I).

From the orientation of I' , note that the sign of the faces alternate around any of these vertices (see Figure 6). We now want to draw G^Δ planarly, in such a way that its inner faces are all homothetic to the triangle formed by following the three vectors \vec{a} , \vec{b} , and \vec{c} . More precisely, for a face f of size α that is bordered by subpaths $P_a^f \subseteq P_{a_i}$, $P_b^f \subseteq P_{b_j}$, and $P_c^f \subseteq P_{c_k}$, the subpaths P_a^f , P_b^f and P_c^f should be mapped to vectors $\alpha \vec{a}$, $\alpha \vec{b}$, and $\alpha \vec{c}$, respectively, in such a way that the edge length along these paths are met. Note that there is no local obstruction to the existence of such embedding.

- Each edge ff' of G^Δ is consistently embedded. Indeed, the length of ff' is set in G^Δ , and regardless of the considered incident face (as these faces have different signs), the vector $\vec{ff'}$ has the same direction.

- For the outer vertices $f_{\vec{a}}^o$, $f_{\vec{b}}^o$, and $f_{\vec{c}}^o$, their incident inner faces form an angle smaller than π (e.g. for $f_{\vec{a}}^o$ the angle is the one from \vec{c} to $-\vec{b}$). For any other outer vertex f , which necessarily corresponds to a single vertex of I' , its (three) incident inner faces form an angle of size exactly π . For example, if f is in the middle of the path P_{a_0} and at the end of paths P_{b_j} and P_{c_k} , we know by (1) that the inner faces incident to P_{a_0} are positive, while the third one is negative because the edges fb_j and fc_k are oriented towards f in I' . Thus, the angles around f go from \vec{a} , to $-\vec{c}$, to \vec{b} , and to $-\vec{a}$.
- For any inner vertex f corresponding to a single vertex of I' , its (four) incident faces form an angle of size exactly 2π . For example, if f is in the middle of a path P_{a_i} and at the end of paths P_{b_j} and P_{c_k} , as the signs of the four faces alternate, the angles around f go from $-x\vec{a}$ to $x\vec{a}$, to $-x\vec{c}$, to $x\vec{b}$, and back to $-x\vec{a}$, for $x \in \{-1, +1\}$.
- Similarly, for an inner vertex f originating from two vertices of I' , the sum of the 6 angles is again 2π .

From these observations, a simple variant of Lemma 6 of [5] ensures the existence of such embedding. Alternatively, one could triangulate G^Δ to use this lemma directly.

Note that this embedding is such that for each vertex $a_i \in V(T)$ (resp. $b_j \in V(T)$ and $c_k \in V(T)$) the corresponding path P_{a_i} (resp. P_{b_j} and P_{c_k}) forms a segment parallel to \vec{a} (resp. \vec{b} and \vec{c}). As in G^Δ a vertex f is in the middle of at most one path P_v , these segments do not cross. For any inner edge of T , say $a_i b_j$ incident to a face $f \in F_2(T)$, the paths P_{a_i} and P_{b_j} touch at the vertex f of G^Δ . For the outer edges the contact points are $f_{\vec{a}}^o$, $f_{\vec{b}}^o$, and $f_{\vec{c}}^o$. We thus have a TC-scheme of T .

If some faces $f \in F_1$ are such that $x_f = 0$, consider a face $a_i b_j c_k \in F_1$ such that $x_{a_i b_j c_k} = 0$. Let a', b', c' be the vertices belonging to a triangle adjacent to $a_i b_j c_k$ (see the left of Figure 7). Note that the vertices a_i and a' (resp. the vertices b_j and b' , and the vertices c_k and c') have at least two common neighbors, b_j, c_k (resp. a_i, c_k and a_i, b_j). It may be the case that they have more common neighbors, but the planarity and the 3-coloring of T forces one of these pairs to restrict to these two common neighbors only. Let us assume that a_i and a' have exactly two common neighbors, b_j, c_k . Let T' be the Eulerian triangulation obtained from T by deleting the edges $b_j c_k$, $a' b_j$ and $a' c_k$, and by merging a_i and a' (see Figure 7). The resulting vertex of T' is denoted by a'_i . Note that by the choice of a_i, a' , T' has no multiple edges. We can thus apply the induction on T' .

Let \mathcal{L}' be the linear system defined for T' . Note that a solution of \mathcal{L} clearly induces a solution of \mathcal{L}' . Indeed, every vertex $v \in V(T') \setminus \{a'_i, b_j, c_k\}$ is incident to the same faces as in T' , so they sum up to 0 (or to 1 for outer vertices). For b_j , or c_k these vertices are incident to one less face of F_1 , the face $a_i b_j c_k$, and as $x_{a_i b_j c_k} = 0$, their incident faces still sum up to 0 (or to 1) in T' . Similarly, as the faces of F_1 incident to a'_i in T' are the faces of F_1 incident to a_i or to a' in T , except $a_i b_j c_k$, they sum up to 0. As the solution of \mathcal{L}' has one less 0 entry, we can apply the induction, and consider a

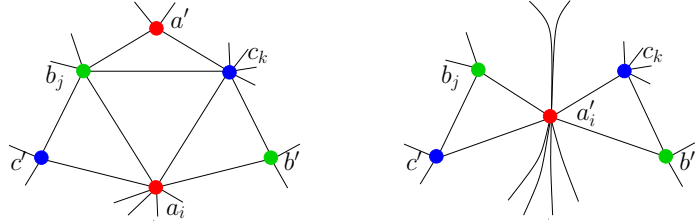


Figure 7: Reduction to a smaller triangulation T' by identifying a_i and a' .

TC-scheme \mathcal{R}' of T' corresponding to this solution of \mathcal{L}' . We consider different cases according to whether a_i and a' have non-zero valued incident faces in T .

If a' has only zero valued incident faces in T , then \mathcal{R}' is also a TC-scheme for T corresponding to \mathcal{L} . Note by Lemma 6.(2) that every non-degenerate inner face f of $C(\mathcal{R}')$ is a face of $F_1(T')$. Renaming a_i the vertex originated by the merging of a_i and a' , instead of a'_i , all the faces of $F_1(T')$ with non-zero size, are also faces of $F_1(T)$. Hence, \mathcal{R}' is also a TC-scheme for T . The fact that it corresponds to \mathcal{L} is clear by the construction.

If a_i has only zero valued incident faces in T , we proceed as above. The only difference is that we have to denote a' the vertex originated by the merging of a_i and a' .

If both a_i and a' have non-zero valued incident faces in T , let us divide the segment a'_i of \mathcal{R}' into two parts, one for each of a_i and a' . Note that the faces of $F_1(T) \setminus \{a_i b_j c_k\}$ incident to a_i (resp. a') in T correspond to consecutive triangles around a'_i . Furthermore, as their sizes sum up to 0 there is a point $p \in a'_i$ that divides a'_i into two parts, a_i and a' , such that the faces of $F_1 \setminus \{a_i b_j c_k\}$ incident to a_i (resp. a') in T correspond to triangles with a side contained inside a_i (resp. a'). Let us denote by \mathcal{R} the obtained TC-representation. As every non-degenerate face f of $C(\mathcal{R})$ corresponds to a face of $F_1(T)$ whose size is x_f , by Lemma 6.(2) we have that \mathcal{R} is a TC-scheme of T following the solution of \mathcal{L} . This concludes the induction step of the proof. \square

4 3-slopes segment representations

In this section, we use Theorem 7 to prove the main theorem of the article, Theorem 1. As already mentioned, it is sufficient to prove it for Eulerian triangulations. From now on, given a Eulerian triangulation with more than three vertices, let a_1, b_1 and c_1 be the vertices forming an inner face with vertices b_0 and c_0 , with a_0 and c_0 , and with a_0 and b_0 , respectively. Theorem 1 follows from the following technical proposition.

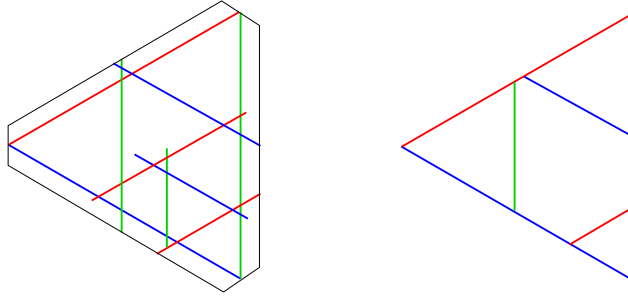


Figure 8: (left) A 3-slopes segment representation inside a hexagon. Note that some intersection points lie inside the triangle $a_0b_0c_0$, while some are outside this triangle (here this is the case for the intersection of b_1 and c_1). (right) An illustration of its shape.

Proposition 12 *For every sufficiently small $\epsilon > 0$, every simple Eulerian triangulation T admits a 3-slopes segment representations \mathcal{R} such that:*

- The segments a_0 , b_0 , and c_0 form a triangle Δ of size 1 (its sides are obtained by following \vec{a} , \vec{b} , and \vec{c}).
- Every segment is contained in the hexagon centered on Δ , obtained by successively following $(1 - \epsilon)\vec{a}$, $-2\epsilon\vec{c}$, $(1 - \epsilon)\vec{b}$, $-2\epsilon\vec{a}$, $(1 - \epsilon)\vec{c}$, and $-2\epsilon\vec{b}$ (see Figure 8).
- The segments a_1 , b_1 , and c_1 have both endpoints on the border of the hexagon.
- No three segments intersect at the same point.
- For every inner edge uv the segments u and v cross each other (i.e. their intersection point is not an endpoint).

Given such representation \mathcal{R} of a triangulation having some inner vertices, we define the *shape* of \mathcal{R} as the triplet (s_a, s_b, s_c) of sizes of the triangles corresponding to $a_1b_0c_0$, $a_0b_1c_0$, $a_0b_0c_1$, respectively, in \mathcal{R} (see the right part of Figure 8).

Proof. We proceed by induction on $|V(T)|$. The initial case of this induction, when $|V(T)| = 3$ clearly holds. We thus proceed to the induction step with a Eulerian triangulation T such that $|V(T)| > 3$, and we assume that the proposition holds for any simple Eulerian triangulation with fewer vertices.

By Theorem 7, we consider a TC-scheme \mathcal{R} of T , and we prolong the segments a_1 , b_1 , and c_1 to have their endpoints on the border of the hexagon. Then, to reach the sought representation, we *resolve* every *degenerate point* of \mathcal{R} . A k -*degenerate point* of \mathcal{R} , for $k = 3, 5$ or 6 , is a point p belonging to k segments. Here, *resolving* means that the segments of a 3-degenerate point (resp. a 5- or a 6-degenerate point) are moved to form a triangle (resp. two triangles, or a polygon) inside which we are going to draw

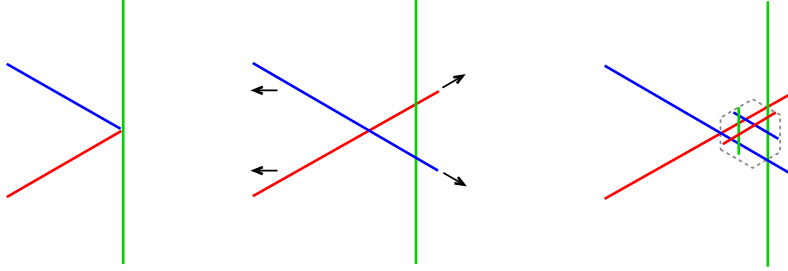


Figure 9: (left) A 3-degenerate point on \mathcal{V} (middle) Small perturbation of \mathcal{R} (right) The addition of a representation roughly inside the new triangle. The new segments are added in the hexagon with dashed gray border.

a 3-slopes representation of the graph corresponding to this degenerate face of $C(\mathcal{R})$, this is possible by using the induction on this smaller graph. The degenerate points of \mathcal{R} are resolved from left to right. This means that at a given stage of this process there is a vertical line (parallel with \overrightarrow{b}) \mathcal{V} such that on its left all the intersection points (except for the one of a_0c_0) are crossing points. This implies that on the left of \mathcal{V} the representation handles some small perturbations: Every segment, except a_0 and c_0 , can slightly move in any direction, without creating or destroying any intersection point.

Let \mathcal{V} be the leftmost vertical line containing degenerate points. We resolve those degenerate points by slightly moving segments on the left of or on \mathcal{V} , while maintaining the right side of the representation unchanged (except at the vicinity of \mathcal{V}). We consider different cases according to the degenerate points on \mathcal{V} .

If \mathcal{V} contains a 3-degenerate point p in the interior of a (vertical) segment b_j and at the end of two segments a_i and c_k lying on the left of \mathcal{V} , the situation is rather simple. Move these segments a_i , c_k a little to the left and slightly prolong them to intersect b_j (see Figure 9). As there is no degenerate point on the left of \mathcal{V} these moves can be done while maintaining the existing intersections and avoiding new intersections. If $a_i b_j c_k$ is not a face of T , consider the triangulation T' induced by the vertices in the cycle $a_i b_j c_k$ of T . By induction, T' has a representation that can be drawn inside a hexagon centered on the newly formed triangle bordered by the segments a_i , b_j and c_k .

If \mathcal{V} contains a 5-degenerate point p in the interior of a (vertical) segment b_j , the situation is similar to the previous one. Move the segments on the left of \mathcal{V} as depicted in Figure 10. If the new triangle is not a face of T , we add a representation inside. We are now left with a single 3-degenerate point at p . This corresponds to the following case.

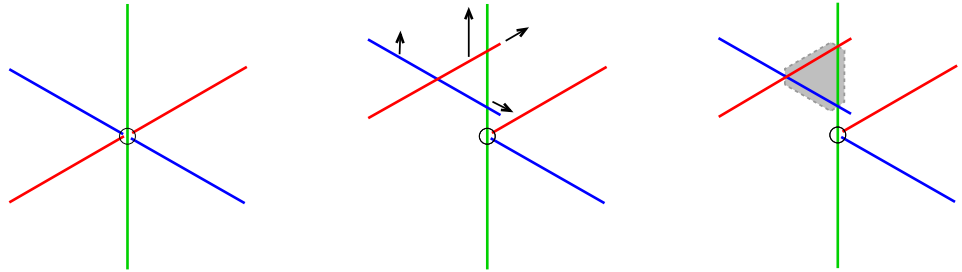


Figure 10: (left) A 5-degenerate point on \mathcal{V} . (middle) A small perturbation of \mathcal{R} . The small circle indicates the position of the original 5-degenerate point \mathbf{p} , that is now a simple 3-degenerate point. (right) Addition of a 3-slope segment representation, if needed.

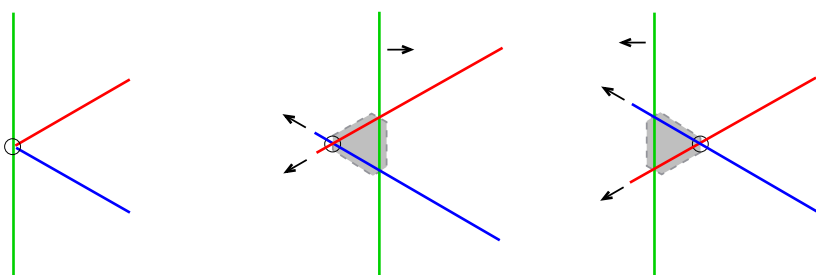


Figure 11: (left) A 3-degenerate point \mathbf{p} , in a small circle, with segments on the right of \mathcal{V} . (middle) Slightly moving \mathbf{b}_j to the right, and addition of extra segments in the hexagon, if needed. (right) Slightly moving \mathbf{b}_j to the left.

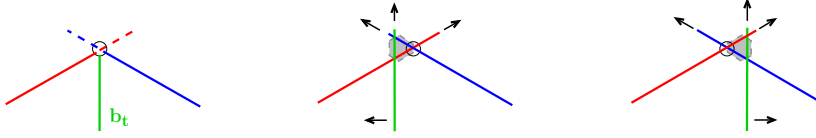


Figure 12: (left) A 3-degenerate point p at the end of b_t . The cases where a_i end at p is similar to the case where c_k ends at this point, since the segment ending there is prolonged. (middle) Slightly moving b_t to the left, and addition of extra segments in the hexagon, if necessary. (right) Slightly moving b_t to the right.

If \mathcal{V} contains a 3-degenerate point p in the interior of a (vertical) segment b_j and at the end of two segments, a_i and c_k , lying on the right of \mathcal{V} , one can move b_j slightly to the right or slightly to the left and resolve these points without changing the right part of the representation. The choice of moving b_j to the right or to the left is explained in the next paragraph, but we can assume this move to be arbitrarily small. Regardless of the direction b_j is moved, one has to prolong a_i and c_k to keep the intersections between these segments and b_j (see Figure 11). Note that in order to preserve the representation on the right of \mathcal{V} the segments a_i and c_k are not moved, they are only prolonged across p . Again, if $a_i b_j c_k$ is not a face of T , we draw a representation inside the newly formed triangle. Note that if b_j moves to the right, the triangle bordered by a_i , b_j and c_k has negative size, but it suffices to apply a homothety with negative ratio to obtain a representation that can be drawn inside.

Consider now the degenerate points at the end of a (vertical) segment b_j of \mathcal{V} . Let b_1, b_2, \dots, b_t be a maximal sequence of segments on \mathcal{V} , from bottom to top, such that b_j and b_{j+1} intersect in a point. We are going to move these segments slightly to the right or slightly to the left of \mathcal{V} . The direction of these moves, right or left, and their exact magnitude will be set later, but remember that these moves can be made arbitrarily small. Recall that the 3-degenerate points in the interior of the segments b_j with $1 \leq j \leq t$ can be dealt if the move of b_j is sufficiently small (see the previous cases).

Consider first the upmost endpoint p of b_t , and let a_i and c_k be the other segments meeting at this point. The point p is an endpoint for one of a_i or c_k . We slightly prolong this segment across p (see Figure 12). Then, whatever the direction b_t is moved, by slightly prolonging b_t , we maintain the desired intersection. Note that these prolongings ensure that the representation on the right of \mathcal{V} is unchanged, such as segment a_0 if $a_i = a_0$. Again, if $a_i b_t c_k$ is not a face of T , we draw a representation inside the newly formed triangle. In this case, if $a_i = a_0$, note that as the move of b_t can be arbitrarily small, the representation of T can remain inside the hexagon of Proposition 12. The case of the lowest endpoint of b_1 is symmetrical.

Now we arbitrarily choose to move b_1 towards the left of \mathcal{V} , and we assume that move to be arbitrarily small. In the following we will see how the direction chosen for this move, to the left, implies a direction for moving b_2 , which in turn implies a direction for moving b_3 , and so on until b_t . Regarding the magnitude of these moves,

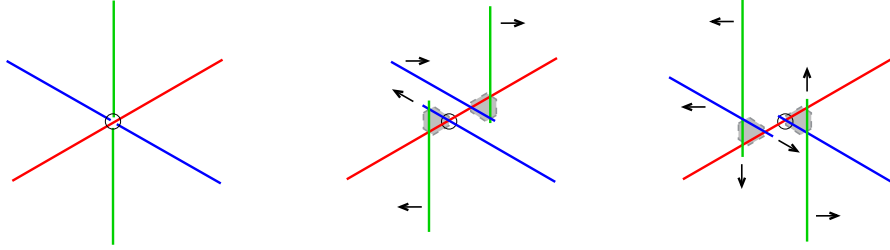


Figure 13: (left) A 5-degenerate point on \mathcal{V} (middle) & (right) Small moves that resolve this point with respect to the directions taken by \mathbf{b}_j and \mathbf{b}_{j+1} .

they are all positively correlated, meaning that all these moves can be arbitrarily small, if the first one (of \mathbf{b}_1) is chosen sufficiently small.

Consider now any intersection point \mathbf{p} between \mathbf{b}_j and \mathbf{b}_{j+1} , and let us distinguish various cases according to the other segments containing \mathbf{p} .

Suppose there is a segment \mathbf{a}_i going through \mathbf{p} . It is shown in Figure 13 how to resolve these two overlapped 3-degenerate points, in order to create two triangles, where one can add a small representation if needed. The case where there is a segment \mathbf{c}_k going through \mathbf{p} is similar.

Assume now that six segments intersect at \mathbf{p} . Let \mathbf{b}_j be the one below \mathbf{p} , and let $\mathbf{a}, \mathbf{c}, \mathbf{b}_{j+1}, \mathbf{a}',$ and \mathbf{c}' be the other ones around \mathbf{p} clockwise. The degenerate face corresponding to \mathbf{p} in $C(\mathcal{R})$ is bounded by the cycle $(b_j, a, c, b_{j+1}, a', c')$, and there are several cases according to whether there are chords within this cycle in T . For all the cases, we assume that the move of \mathbf{b}_j , its direction and its (arbitrarily small) magnitude is set, and we will see how it determines the direction and magnitude of the moves applied to $\mathbf{a}, \mathbf{c}, \mathbf{b}_{j+1}, \mathbf{a}',$ and \mathbf{c}' .

Suppose that none of $ab_{j+1}, b_{j+1}c'$, or ac' is a chord of $(b_j, a, c, b_{j+1}, a', c')$ in T (see Figure 14), then we consider the subgraph of T induced by the vertices on and inside this cycle. We add the edges $ab_{j+1}, b_{j+1}c'$, and ac' outside the cycle, and we denote by T' the obtained simple Eulerian triangulation. By the induction, we know that T' admits a 3-slope segment representation \mathcal{R}' , and let (s_a, s_b, s_c) be the shape of \mathcal{R}' . If \mathbf{b}_j is moved to the left of \mathcal{V} , we resolve the point \mathbf{p} by moving the segments as depicted in Figure 14. Each of these moves are proportional to the move of \mathbf{b}_j towards the left, and the magnitude of each of these moves is prescribed by the shape (s_a, s_b, s_c) in order to allow us to copy \mathcal{R}' inside the triangle formed by $\mathbf{a}, \mathbf{b}_{j+1},$ and \mathbf{c}' . Then we shorten $\mathbf{a}, \mathbf{b}_{j+1},$ and \mathbf{c}' to avoid intersections among them. The case where \mathbf{b}_j is moved to the right of \mathcal{V} is depicted in the left of Figure 15. In that case, note that \mathcal{R}' is not only rescaled to fit into the hexagon, but we first consider a homothety of \mathcal{R}' with negative ratio.

If none of $b_jc, ca',$ or $a'b_j$ is a chord of $(b_j, a, c, b_{j+1}, a', c')$ we proceed similarly (see the middle and the right of Figure 15). The only difference is that we add the edge $b_jc, ca',$ or $a'b_j$ outside $(b_j, a, c, b_{j+1}, a', c')$ to obtain T' .

We now have to deal with the case where $(b_j, a, c, b_{j+1}, a', c')$ has two opposite

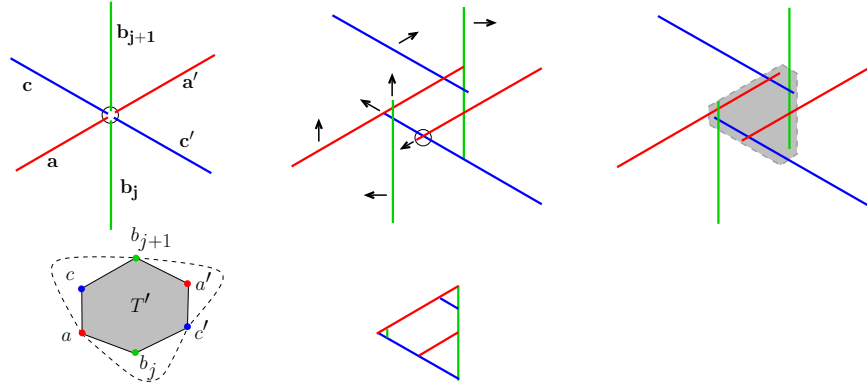


Figure 14: Resolution of a 6-degenerate point p when there is no chord ab_{j+1} , $b_{j+1}c'$, or ac' . (left) A 6-degenerate point on \mathcal{V} , and below, the triangulation T' obtained from the vertices inside this degenerate face of the TC-scheme. (middle) The shape of \mathcal{R}' and the moves made according to this shape and according to the move of b_j towards the left. (right) The 3-slope segment representation \mathcal{R}' is included, and the segments a , b_{j+1} , and c' are shortened to avoid the artificially added edges ab_{j+1} , $b_{j+1}c'$, and ac' .

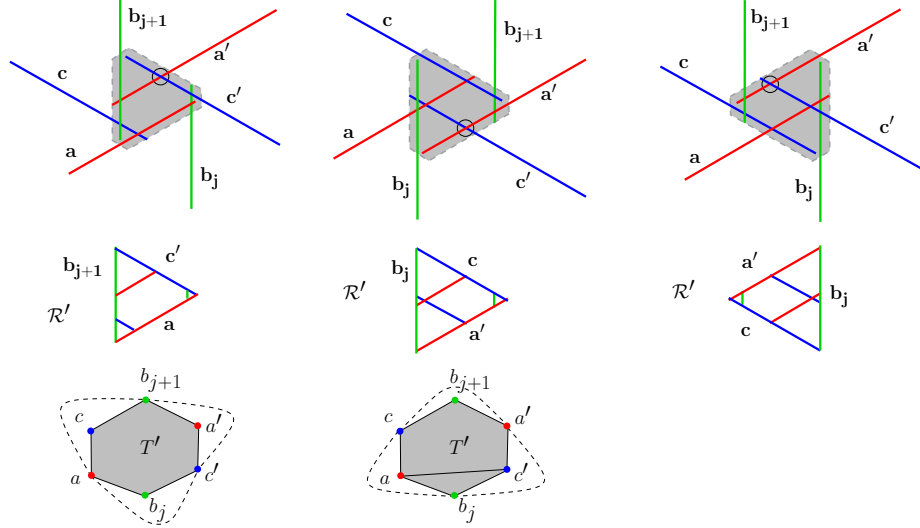


Figure 15: (left) Resolution of a 6-degenerate point p when there is no chord ab_{j+1} , $b_{j+1}c'$, or ac' , and when b_j is moved to the right. (middle) The case where none of b_jc , ca' , or $a'b_j$ is a chord and where b_j is moved to the left. In this illustration there is a chord ac' , but this may not be the case, of course. (right) Same case with b_j moved to the right of p .

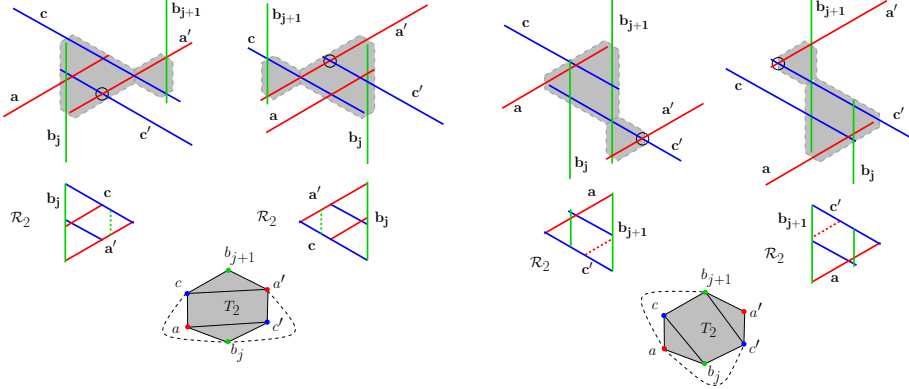


Figure 16: (left) The case where ac' and $a'c$ are chords, with b_j moved to the left or to the right of p . (right) The case where b_jc and $b_{j+1}c'$ are chords, with b_j moved to the left or to the right of p . In the first case, note that \mathcal{R}_2 contains the intersection point of a and c' inside the triangle, but it could be the case that the representation \mathcal{R}_2 obtained by induction has this intersection point located outside the triangle. See for example the illustration on the right part, where the intersection point of b_j and c is outside the triangle.

chords. If ac' and $a'c$ are chords (see the left part of Figure 16), we consider two triangulations. Let T_1 be the one inside the cycle (c, b_{j+1}, a') and let T_2 be the one obtained from the interior of the 5-cycle (a', c', b_j, a, c) by adding the edges $a'b_j$ and b_jc outside. By the induction, we know that T_1 and T_2 admit 3-slopes segment representations \mathcal{R}_1 , and \mathcal{R}_2 . We resolve the point p by moving the segments as depicted in Figure 16, and the magnitude of each of these moves, except for b_j and b_{j+1} , is prescribed by the shape of \mathcal{R}_2 . Then we shorten two segments to avoid the intersections corresponding to $a'b_j$ and b_jc . The segment b_{j+1} is moved away to avoid the interior of the hexagon containing \mathcal{R}_2 . Then \mathcal{R}_1 is drawn inside the triangle bordered by b_{j+1}, a' and c . This is possible because the hexagons containing \mathcal{R}_1 and \mathcal{R}_2 do not overlap.

If b_jc and $b_{j+1}c'$ are chords, we proceed similarly (see the right part of Figure 16). The difference is that, here, T_1 is the triangulation inside the cycle (b_{j+1}, a', c') and let T_2 be the one obtained from the interior of the 5-cycle (c', b_j, a, c, b_{j+1}) by adding the edges ab_{j+1} and ac' outside.

If ab_{j+1} and $a'b_j$ are chords, we proceed similarly (see Figure 17). One difference is that, T_1 is the triangulation inside the cycle (a, c, b_{j+1}) and that T_2 is the one obtained from the interior of the 5-cycle $(b_{j+1}, a', c', b_j, a)$ by adding the edges ac' and $b_{j+1}c'$. Another difference is that we proceed differently according to the shape of \mathcal{R}_2 . We distinguish the case where the intersection point of a' and b_j lies inside the triangle $ab_{j+1}c'$ or outside it.

Finally, note that the moves of b_j and b_{j+1} are of proportional magnitudes (up to some constant depending on the shapes of \mathcal{R}' or \mathcal{R}_2). This property propagates from b_1 , to b_t , and it is thus possible to assume that all these moves are arbitrarily small. The procedure hence leads to the sought 3-slope segment representation, and

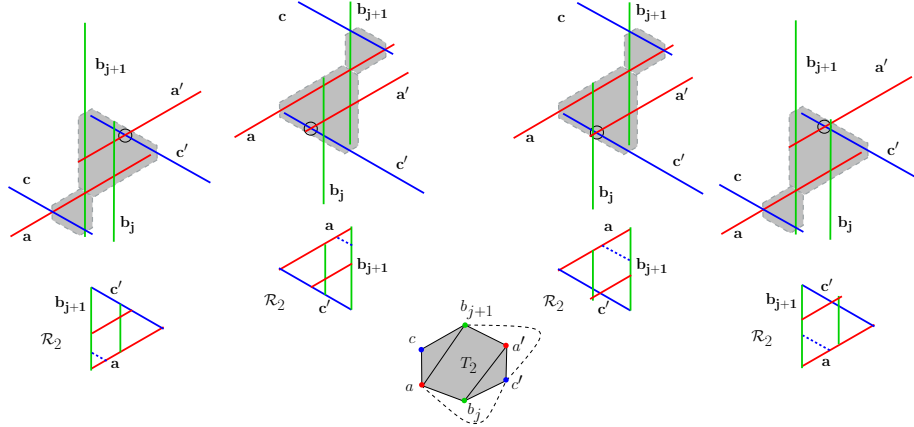


Figure 17: The case where ab_{j+1} and $a'b_j$ are chords. (left) If in \mathcal{R}_2 , the intersection point of a' and b_j is inside the triangle $ab_{j+1}c'$. The two subcases whether b_j is moved to the left or to the right of p . (right) If in \mathcal{R}_2 , the intersection point of a' and b_j is outside the triangle $ab_{j+1}c'$.

this concludes the proof of the proposition. \square

5 Conclusion

Our result implies that for $k \leq 3$, planar graphs that are k -colorable admit a k -slopes segment representation, where parallel segments induce an independent set. These graphs have a so-called *PURE- k -DIR* representation. Unfortunately, this does not extend to the final case $k = 4$ as conjectured by D. West [18]. The author [9] built a counter-example based on a construction of Kardoš and Narboni [12]. Their construction is an example of a signed planar graph that is not 4-colorable, in the sense of signed graphs. However, it remains open to know whether (4-colorable) planar graphs admit a *PURE- k -DIR* representation (resp. a non-necessarily pure one) for some $k > 4$ (resp. $k > 2$).

Acknowledgements. The author is thankful to the anonymous reviewers, especially for a simplified proof of Lemma 8, and for pointing out a gap in a preliminary version of the proof. The author is also thankful to Pascal Ochem for bringing [12] to his attention, and to Marc de Visme for fruitful discussions on this topic.

References

- [1] N. de Castro, F. Cobos, J.C. Dana, A. Márquez, and M. Noy. Triangle-free planar graphs as segment intersection graphs. *J. Graph Algorithms Appl.*, 6(1):7–26, 2002.

- [2] J. Chalopin and D. Gonçalves. Every planar graph is the intersection graph of segments in the plane: extended abstract. *Proceedings of the forty-first annual ACM symposium on Theory of computing*, 631–638, 2009.
- [3] J. Czyzowicz, E. Kranakis, and J. Urrutia. A simple proof of the representation of bipartite planar graphs as the contact graphs of orthogonal straight line segments. *Inform. Process. Lett.*, 66(3):125–126, 1998.
- [4] S. Felsner. Triangle Contact Representations. *Midsummer Combinatorial Workshop*, 2009.
- [5] S. Felsner, H. Schrezenmaier, and R. Steiner. Equiangular Polygon Contact Representations. *Proc. of WG 2018, LNCS* 11159:203–215, 2018. (Long version retrieved at <http://page.math.tu-berlin.de/~felsner/Paper/kgons.pdf>)
- [6] H. de Fraysseix and P. Ossona de Mendez. Representations by Contact and Intersection of Segments. *Algorithmica*, 47:453–463, 2007.
- [7] H. de Fraysseix, P. Ossona de Mendez, and J. Pach. Representation of planar graphs by segments. *Intuitive geometry (Szeged, 1991), Colloq. Math. Soc. János Bolyai*, 63:109–117, 1994.
- [8] D. Gonçalves. 3-colorable planar graphs have an intersection segment representation using 3 slopes. *Proc. of WG 2019, LNCS* 11789:351–363, 2019.
- [9] D. Gonçalves. Not all planar graphs are in PURE-4-DIR. *J. of Graph Algorithms and Applications*, 24(3):293–301, 2020.
- [10] D. Gonçalves, L. Isenmann, and C. Pennarun. Planar Graphs as L-intersection or L-contact graphs. *Proc. of SODA 2018*, 172–184, 2018.
- [11] I.B.-A. Hartman, I. Newman, and R. Ziv. On grid intersection graphs. *Discrete Math.*, 87(1):41–52, 1991.
- [12] F. Kardoš, and J. Narboni. On the 4-color theorem for signed graphs. *Eur. J. of Combinatorics*, 91, 103215, 2021.
- [13] J. Kratochvíl. String graphs. II. Recognizing String Graphs is NP-hard. *J. Combin. Theory. Ser. B*, 52:67–78, 1991.
- [14] L. Lovász. Combinatorial problems and exercises. *American Mathematical Soc.*, 1993.
- [15] E.R. Scheinerman. Intersection classes and multiple intersection parameters of graphs. *PhD Thesis, Princeton University*, 1984.
- [16] E.R. Scheinerman. *Private communication to D. West*.
- [17] L. Stockmeyer. Planar 3-colorability is polynomial complete. *ACM SIGACT News* 5(3):19–25, 1973.
- [18] D. West. Open problems. *SIAM J. Discrete Math. Newslett.*, 2(1):10–12, 1991.